


## Spin-orbit torque in perpendicularly magnetized [Pt/Ni] multilayers

Ying Cao(曹颖), Zhicheng Xie(谢志成), Zhiyuan Zhao(赵治源), Yumin Yang(杨雨民), Na Lei(雷娜), Bingfeng Miao(缪冰锋), and Dahai Wei(魏大海)
**Citation:**Chin. Phys. B, 2023, 32 (**10**): 107507. DOI: 10.1088/1674-1056/acee57
Journal homepage: http://cpb.iphy.ac.cn; http://iopscience.iop.org/cpb

**What follows is a list of articles you may be interested in**

---

## Topological magnetotransport and electrical switching of sputtered antiferromagnetic $Ir_{20}Mn_{80}$

Danrong Xiong(熊丹荣), Yuhao Jiang(蒋宇昊), Daoqian Zhu(朱道乾), Ao Du(杜奥), Zongxia Guo(郭宗夏), Shiyang Lu(卢世阳), Chunxu Wang(王春旭), Qingtao Xia(夏清涛), Dapeng Zhu(朱大鹏), and Weisheng Zhao(赵巍胜)
Chin. Phys. B, 2023, 32 (**5**): 057501. DOI: 10.1088/1674-1056/acb9ec

## Orbital torque of Cr-induced magnetization switching in perpendicularly magnetized Pt/Co/Pt/Cr heterostructures

Hongfei Xie(谢宏斐), Yuhan Chang(常宇晗), Xi Guo(郭玺), Jianrong Zhang(张健荣), Baoshan Cui(崔宝山), Yalu Zuo(左亚路), and Li Xi(席力)
Chin. Phys. B, 2023, 32 (**3**): 037502. DOI: 10.1088/1674-1056/aca6d7

## Skyrmion-based logic gates controlled by electric currents in synthetic antiferromagnet

Linlin Li(李林霖), Jia Luo(罗佳), Jing Xia(夏静), Yan Zhou(周艳), Xiaoxi Liu(刘小晰), and Guoping Zhao(赵国平)
Chin. Phys. B, 2023, 32 (**1**): 017506. DOI: 10.1088/1674-1056/ac9b01

## Enhancement of spin-orbit torque efficiency by tailoring interfacial spin-orbit coupling in Pt-based magnetic multilayers

Wenqiang Wang(王文强), Gengkuan Zhu(朱耿宽), Kaiyuan Zhou(周恺元), Xiang Zhan(战翔), Zui Tao(陶醉), Qingwei Fu(付清为), Like Liang(梁力克), Zishuang Li(李子爽), Lina Chen(陈丽娜), Chunjie Yan(晏春杰), Haotian Li(李浩天), Tiejun Zhou(周铁军), and Ronghua Liu(刘荣华)
Chin. Phys. B, 2022, 31 (**9**): 097504. DOI: 10.1088/1674-1056/ac76aa

## Probing the magnetization switching with in-plane magnetic anisotropy through field-modified magnetoresistance measurement

Runrun Hao(郝润润), Kun Zhang(张昆), Yinggang Li(李迎港), Qiang Cao(曹强), Xueying Zhang(张学莹), Dapeng Zhu(朱大鹏), and Weisheng Zhao(赵巍胜)
Chin. Phys. B, 2022, 31 (**1**): 017502. DOI: 10.1088/1674-1056/ac21bb

---

**RAPID COMMUNICATION**

# Spin–orbit torque in perpendicularly magnetized [Pt/Ni] multilayers

Ying Cao(曹颖)[1,2], Zhicheng Xie(谢志成)[1,2], Zhiyuan Zhao(赵治源)[1,2], Yumin Yang(杨雨民)[1,2], Na Lei(雷娜)[3,†], Bingfeng Miao(缪冰锋)[4], and Dahai Wei(魏大海)[1,2,‡]

[1] *State Key Laboratory for Superlattices and Microstructures, Institute of Semiconductors, Chinese Academy of Sciences, Beijing* 100083, *China*
[2] *College of Materials Science and Opto-Electronic Technology, University of Chinese Academy of Sciences, Beijing* 100049, *China*
[3] *Fert Beijing Institute, MIIT Key Laboratory of Spintronics, School of Integrated Circuit Science and Engineering, Beihang University, Beijing* 100191, *China*
[4] *National Laboratory of Solid State Microstructures and Department of Physics, Nanjing University, Nanjing* 210093, *China*

(Received 25 June 2023; revised manuscript received 19 July 2023; accepted manuscript online 9 August 2023)

The performance of spin–orbit torque (SOT) in heavy metal/ferromagnetic metal periodic multilayers has attracted widespread attention. In this paper, we have successfully fabricated a series of perpendicular magnetized $[Pt(2-t)/Ni(t)]_4$ multilayers, and studied the SOT in the multilayers by varying the thickness of Ni layer $t$. The current induced magnetization switching was achieved with a critical current density of $1\times10^7$ A/cm$^2$. The damping-like SOT efficiency $\xi_{DL}$ was extracted from an extended harmonic Hall measurement. We demonstrated that the $\xi_{DL}$ can be effectively modulated by $t_{Pt}/t_{Ni}$ ratio of Pt and Ni in the multilayers. The SOT investigation about the $[Pt/Ni]_N$ multilayers might provide new material candidates for practical perpendicular SOT-MRAM devices.

**Keywords:** spin–orbit torque, perpendicular magnetic anisotropy, spintronics

**PACS:** 75.70.Tj, 75.30.Gw, 75.50.Ss, 72.25.Ba **DOI:** 10.1088/1674-1056/acee57

## 1. Introduction

The rapid development of emerging information technologies, such as artificial intelligence, requires high-performance and energy-efficient memory devices.[1,2] The spintronic memories, where information is encoded by the magnetization, provide a promising solution for the next generation data storage and processing.[3] Magnetic films exhibiting perpendicular magnetic anisotropy (PMA) are of great significance in the fabrication of magnetic tunnel junctions (MTJs),[4] which are the core of the magnetic random-access memory (MRAM) with high storage density and high thermal stability at room temperature.[5,6] Meanwhile the spin–orbit torque (SOT) MRAM has advantages of high energy efficiency, sub-ns switching and high endurance for writing operation.[7,8] These advancements have been pivotal in driving forward research and development efforts, enabling integration with traditional complementary metal–oxide–semiconductor (CMOS) processes.[9] Thus, the magnetic materials and structures with both strong PMA and high SOT efficiency are crucial for the development of the MRAM applications.

The perpendicular magnetized CoFeB/MgO bilayer is one of the most promising MTJ materials systems, which has been intensively investigated and widely utilized in various spintronics applications.[10] However, the interfacial PMA originated from the CoFeB/MgO interface is insufficient to maintain high thermal stability for MTJs at reduced dimension smaller than 20 nm.[11,12] To achieve stronger PMA for future sub-10 nm technology node, a number of material systems, such as Co(Tb,Gd),[13,14] $L1_0$-ordered FePt,[15] MnGa[16] alloys and CoPt[17] multilayers have been explored, which have significant magnetocrystalline anisotropy. The bulk PMA in such alloys is very sensitive to the crystal structures of the films, and requires epitaxial growth or strict heat treatment.[18] In contrast, the PMA in the multilayers mainly arises from the interfacial effect at the multiple interfaces which can be easily tuned and are much easier for fabrication in practical device applications.[19] The perpendicular magnetized Co/(Pt, Pd)[20] and Fe/Pt[21] have been realized and intensively studied. However, the PMA of Ni/Pt multilayer is relatively complex. There may be several mechanisms, like the magnetoelastic anisotropy induced by lattice stress[22] and magnetocrystalline anisotropy of the interfaces,[23] that can lead to PMA in Ni/Pt multilayers. Therefore, the dependence of PMA for Ni/Pt multilayer on the thickness of the Ni and Pt layer is intriguing.

Furthermore, the magnetization switching of ferromagnets through current-induced spin–orbit torque (SOT) has received significant attention in recent years.[24] In ferromagnetic metal (FM)/ heavy metal (NM) heterostructures, it is

†Corresponding author. E-mail: na.lei@buaa.edu.cn
‡Corresponding author. E-mail: dhwei@buaa.edu.cn

© 2023 Chinese Physical Society and IOP Publishing Ltd 

mainly the spin Hall effect (SHE) and the inverse spin galvanic effect that provide SOT.[25] When the FM layer exhibits perpendicular magnetic anisotropy, achieving deterministic magnetization switching under current-induced SOT often requires an in-plane bias field to break the symmetry.[26] However, there have been few reports on the SOT of Ni/Pt multilayer films before. This urgently requires us to further explore SOT in Ni/Pt multilayer, in particular, the SOT efficiency and bias field dependence, which could enrich the content of Ni/Pt multilayer films in the field of SOT.

Here we fabricated a multilayer structure composed of $[\mathrm{Pt}(2-t)/\mathrm{Ni}(t)]_4$, where the thickness $t$ of the Ni layer in the periodic layer was adjusted to achieve PMA within a relatively narrow range of thicknesses (below the intrinsic spin diffusion length). The observed PMA phenomenon arises from the interplay between magnetoelastic anisotropy and interface anisotropy. Subsequently, we successfully achieved SOT induced switching of the PMA magnetic multilayer films using a current density of approximately $1\times10^7$ A/cm$^2$. The effectiveness of the spin switching process in the device was found to be influenced by the regulation of the thickness $t$.

## 2. Experimental details

In this work, a serials of substrate/Ge(3)/$[\mathrm{Pt}(2-t)/\mathrm{Ni}(t)]_4$/Ge(3) multilayers were grown on thermally oxidized Si substrates using a high vacuum magnetron sputtering system with a base pressure of $8\times10^{-8}$ Torr at room temperature, as shown by the inset in Fig. 1(a). The $[\mathrm{Pt}(2-t)/\mathrm{Ni}(t)]_4$ multilayers were deposited by the alternative deposition of Pt and Ni using radio-frequency and direct current sputterings. The deposition rates for Pt and Ni are 0.019 nm/s and 0.018 nm/s, respectively, which were calibrated by atomic force microscopy (AFM). The thickness $t$ is varied from 1.45 nm to 1.85 nm. Both buffer and capping layer are 3 nm Ge layers. The AFM measurements also indicate smooth surfaces and the surface root mean square roughness is about 0.3 nm for our stacks. These multilayers were further fabricated into $10\times40$ μm$^2$ Hall bar devices using photolithography and ion milling. The electric transport measurements were performed by a Quantum Design physical property measurement system (PPMS) at room temperature, figure 1(a) illustrates the testing geometry. The magnetic properties of all multilayers were characterized by a Quantum Design magnetic property measurement system (MPMS) with a superconducting quantum interference device (SQUID) at room temperature.

Figure 1(b) exhibits the anomalous Hall loops of the $[\mathrm{Pt}(2-t)/\mathrm{Ni}(t)]_4$ multilayers with different $t$. The multilayers with thicker Ni layers, as shown by the blue ($t = 1.65$), red ($t = 1.75$), and black ($t = 1.85$) curves, exhibit square-shaped loops, which suggest a strong PMA. Otherwise, these multilayers with $t < 1.65$ exhibit in-plane magnetic anisotropy (IMA). The anomalous Hall effect (AHE) coefficients of these multilayers are all negative, which is consistent with the previous results for Ni.[27] The saturation magnetization ($M_\mathrm{S}$) of all multilayers was obtained from the $M$–$H$ hysteresis loops and plotted as black triangles in the top panel of Fig. 1(c). The $M_\mathrm{S}$ monotonically increases with Ni thickness $t$. The magnetic moment per Ni atom was calculated and plotted as the red triangles. It increases from 0.129 $\mu_\mathrm{B}$/atom at $t = 1.45$ nm to 0.216 $\mu_\mathrm{B}$/atom at $t = 1.85$ nm, which is far below the bulk value of Ni ($\sim 0.6$ $\mu_\mathrm{B}$/atom).[23] Such a small atomic moment at room temperature can be attributed to the reduced Curie temperature ($T_\mathrm{C}$) as Ni film in ultrathin region. It increases with thickness $t$ and would finally reach the bulk value for thick Ni films.[23] Notably, the multilayer $[\mathrm{Pt}(2-t)/\mathrm{Ni}(t)]_N$ can show room temperature ferromagnetism only when $N > 3$, while for smaller $N$ the reduced $T_\mathrm{C}$ is lower than room temperature due to the small total thickness of Ni layer.

To investigate the relation between PMA and $t$ in $[\mathrm{Pt}(2-t)/\mathrm{Ni}(t)]_4$ multilayer films, both in-plane and out-of-plane hysteresis loops were measured to extract the values of the effective anisotropy field ($H_\mathrm{K}$). Then, the effective perpendicular magnetic anisotropy energy density ($K_\mathrm{eff}$) was further calculated from the in-plane and out-of-plane hysteresis loops. $H_\mathrm{K}$ (black squares) and $K_\mathrm{eff}$ (red circles) are plotted as a function of $t$ in the middle panel of Fig. 1(c). Consistent with the anomalous Hall loops shown in Fig. 1(b), $K_\mathrm{eff}$ is positive as a perpendicular magnetic anisotropy at $t \geq 1.65$ and presents a nonmonotonic trend with the maximum $K_\mathrm{eff} = 8.21$ kJ/m$^3$ appearing at $t = 1.75$.

The resistivity increases as the thickness decreases due to the additional scattering at the interface and surface of the film. The resistivity ($\rho_{xx}$) of $[\mathrm{Pt}(2-t)/\mathrm{Ni}(t)]_4$ multilayer, composed as $\frac{2}{\rho_{xx}} = \frac{2-t}{\rho_\mathrm{Pt}} + \frac{t}{\rho_\mathrm{Ni}}$ linearly decreases from 90.8 μΩ·cm at $t = 1.45$ to 61.36 μΩ·cm at $t = 1.85$, as shown in Fig. 1(c), which is due to the increase of Ni atoms with $t$. This means that as $t$ increases, the proportion of Ni increases, and the resistance gradually approaches the resistivity of the Ni layer, resulting in a decrease in the total resistivity. The multilayer structure can also be viewed as incorporating Pt intercalation into the Ni layer, which introduces interlayer impurity scattering, and subsequently enhances the resistivity of the material. Although the anomalous Hall resistivity ($\rho_\mathrm{AH}$) should be proportional to $\rho_{xy}$, $\rho_\mathrm{AH}$ is factually inversely proportional to $\rho_{xy}$ with increasing $t$, which is mainly due to the huge enhancement of $M_\mathrm{S}$ related with increasing $t$.

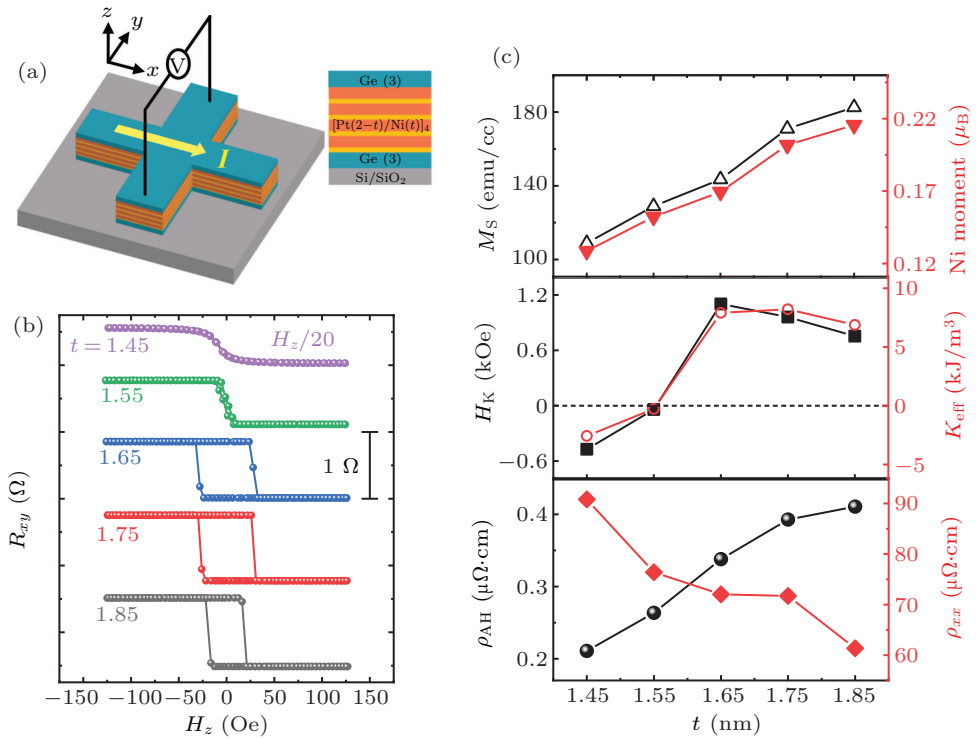



**Fig. 1.** (a) The structure of the $[Pt(2-t)/Ni(t)]_4$ multilayers and the Hall bar device used for the electrical transport measurements. (b) $R_{AH}$ vs. $H_z$ curves of the $[Pt(2-t)/Ni(t)]_4$ multilayers at different $t$. (c) The $t$ dependence of the saturation magnetization ($M_S$), coercive field ($H_C$), anisotropic field ($H_K$), anomalous Hall resistivity ($\rho_{xy}$), and resistivity ($\rho_{xx}$).

## 3. Results and discussion

### 3.1. Current-driven switching of magnetization for the PMA $[Pt(2-t)/Ni(t)]_4$ multilayer

We investigated the current-driven magnetization switching for the $[Pt(2-t)/Ni(t)]_4$ multilayers with PMA from $t = 1.65$ to $t = 1.85$. A series of current pulses with a 50 μs duration are applied to the Hall bar device along the $x$ direction. The in-plane bias field ($H_x$) is necessary to be applied along with the current, which can assist in deterministic magnetization switching. Figure 2(a) shows the current-driven magnetization switching curves for the $[Pt(2-t)/Ni(t)]_4$ multilayer at $t = 1.65$ with $H_x$ from −800 Oe to 800 Oe, which exhibit clockwise and counterclockwise polarity with positive and negative $H_x$, respectively. This is opposite to that of Pt/Co bilayer, which is due to the negative anomalous Hall coefficient of Ni compared with the positive anomalous Hall coefficient of Co.[28]

Furthermore, the critical current density ($J_C$) as a function of $H_x$ with different $t$ is shown in Fig. 2(b), which decreases monotonically with the increase of $|H_x|$. This is because $J_C$ is expressed as[29]

$$J_C = \frac{e\mu_0 M_S t_{FM}\left(H_K - \sqrt{2}|H_x|\right)}{\hbar\xi_{DL}}, \tag{1}$$

where $e$, $\mu_0$, $t_{FM}$, $\hbar$ and $\xi_{DL}$ are the elementary charge, the permeability of vacuum, the thickness of the magnetic layer, the reduced Plank constant, and the damping-like SOT efficiency, respectively. Of course, the current-driven magnetization switching amplitude ($R_{xy}/R_{AH}$) also decreases, when the magnetization of $[Pt(2-t)/Ni(t)]_4$ multilayer is gradually pulled into the $x$–$y$ plane with $|H_x|$ increasing. Because $R_{xy}$ is dependent on the magnetization of the $z$ component.[30]

We note that the current-driven magnetization switching of $[Pt(2-t)/Ni(t)]_4$ multilayer can be achieved even under the residual field (∼ 10 Oe) of the PPMS, which might accidentally be mistaken as field-free current-driven magnetization switching. However, this is actually a significant advantage in spintronic application, because even a tiny $H_x$ can break the symmetry in SOT process. We believe that the main reason should be that the Dzyaloshinskii–Moriya interaction (DMI) of $[Pt(2-t)/Ni(t)]_4$ multilayer is very small. It is well known that DMI represents an obstacle for current-driven magnetization switching.[31]

Subsequently, the thermal stability is estimated by the thermal stability factor $\Delta_T = K_{u,eff}V_{FM}/(k_BT)$, considering a cylinder with typical diameter of 28 nm for MRAM nodes.[32] $\Delta_T$ of these PMA $[Pt(2-t)/Ni(t)]_4$ multilayers are on the same order of magnitude as the previously reported $\Delta_T$ of the applicable MRAM.[5] Obviously, our $[Pt(2-t)/Ni(t)]_4$ multilayer maintains the thermal stability and meets some application standards, which can be further optimized by MgO capping layer for practical applications. Therefore, $[Pt(2-t)/Ni(t)]_4$ multilayer indeed enriches the material system in the field of SOT.

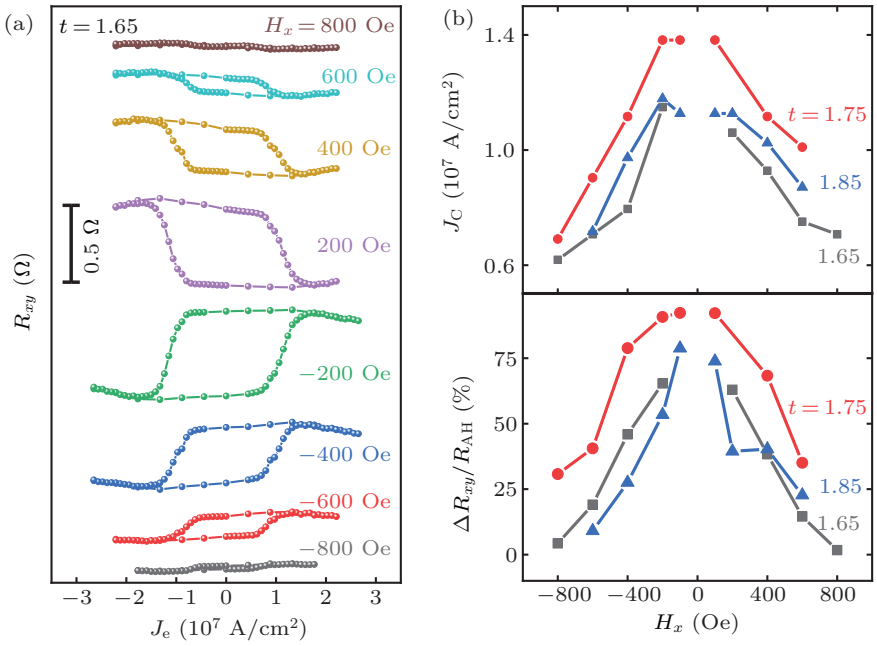



**Fig. 2.** (a) The current-driven switching of magnetization for the $[Pt(2-t)/Ni(t)]_4$ multilayer at $t = 1.65$ with different $H_x$. (b) The $H_x$ dependence of $J_C$ and $\Delta R_{xy}/R_{AH}$.

### 3.2. The harmonic Hall measurements

Next, in order to directly evaluate the current-driven magnetization switching for the $[Pt(2-t)/Ni(t)]_4$ multilayers, we quantified the damping-like SOT efficiency ($\xi_{DL}$) by employing the extended harmonic Hall measurement. The harmonic Hall measurement geometry is shown in Fig. 3(a). A sinusoidal current with a frequency of 521 Hz was applied along the $x$ direction, and then the second harmonic Hall resistances ($R_{2\omega}$) were obtained under a constant external magnetic field ($H_{ext}$) rotating in the $x$–$y$ plane. The azimuthal angle ($\varphi$) is between $H_{ext}$ and the current. The $\varphi$ dependence of $R_{2\omega}$ for the $[Pt(2-t)/Ni(t)]_4$ multilayers at $t = 1.65$ is shown in Fig. 3(b) under a series of $H_{ext}$. Usually, the second harmonic Hall resistances $R_{2\omega}$ can be expressed as[33]

$$R_{2\omega} = -\left(R_{AH}\frac{H_{DL}}{H_{ext}-H_K}+R^0_{\Delta T}\right)\cos\varphi + 2R_{PH}\left(2\cos^3\varphi-\cos\varphi\right)\frac{H_{FL}+H_{Oe}}{H_{ext}}, \quad (2)$$

where $R_{AH}$ is the anomalous Hall resistance, $H_{DL}$ is the damping-like SOT effective field, $H_K$ is the effective anisotropy field , defined as $H_K = H_{ani} - H_{dem}$, with $H_{ani}$ and $H_{dem}$ being the anisotropy field and the demagnetization field, respectively, $R_{PH}$ is the planar Hall resistance, $H_{FL}$ is the field-like SOT effective field, and $H_{Oe}$ is the Oersted field. $R^0_{\Delta T}$ is the thermoelectric contribution for $R_{2\omega}$, which needs to be ruled out.

According to Eq. (2), we calculated and plotted the $-R_{[\cos\varphi]}/R_{AH}$ vs. $1/(H_{ext}-H_K)$ curves under different $H_{ext}$, the damping-like field ($H_{DL}$) was obtained as the slope of linear fitting, as shown in Fig. 3(c). Furthermore, $\xi_{DL}$ was calculated by[34]

$$\xi_{DL} = \frac{2eM_S t_{FM}}{\hbar}\frac{\mu_0 H_{DL}}{J_e}, \quad (3)$$

where $J_e$ is the current density of the Pt layer. Here, we assume that all Pt land Ni layers are simplified as Pt/Ni bilayer. The variation of $\xi_{DL}$ as a function of $t$ is plotted in Fig. 3(d), which shows an almost decreasing trend. It reveals a noticeable trend: $\xi_{DL}$ in the $[Pt\ (2-t)/Ni(t)]_4$ multilayer diminishes rapidly from 0.125 ($t = 1.55$ nm) to 0.035 ($t = 1.85$ nm). This observation indicates a direct influence of the thickness $t$ of the Pt layer in the periodic structure on the SOT of the multilayer film. In the $[Pt(2-t)/Ni(t)]_4$ configuration, two SOT sources contribute to the damping torque: the bulk spin Hall effect (SHE) in the Pt layer and the Rashba effect at the Pt/Ni interface.[26] In typical bilayer film systems such as Pt/Co, Pt/Fe, and Pt/Ni, the generation of damping-like torque is originated from the SHE of the Pt layer in the specific context of SHE. Consequently, it follows that the thickness of the Pt layer directly affects $\xi_{DL}$ in the Pt/Ni multilayer structure.[23]

We have completely adopted a Pt/Ni bilayer in the above description and discussion, just like the classical Pt/Co bilayer in the specific context of SHE. However, the original consideration as Pt/Ni bilayer is not very accurate, as our $[Pt(2-t)/Ni(t)]_4$ multilayer seems to be more similar to a PtNi alloy in terms of material preparation, although the corresponding properties can be well explained considering as Pt/Ni bilayer. But if $[Pt(2-t)/Ni(t)]_4$ multilayer is simply regarded as a PtNi alloy, it is difficult to explain the significant current driven magnetization switching and $\xi_{DL}$ in $[Pt(2-t)/Ni(t)]_4$ multilayer. Because there should be no net spin current flowing in a uniform PtNi alloy. We think that the main reason is

that the film quality gradient always exists in the $z$-direction, which leads to the net SOT in $[\mathrm{Pt}(2-t)/\mathrm{Ni}(t)]_4$ multilayer. Because the contribution of Pt/Ni at the lower interface to SOT is always greater than that of Ni/Pt at the upper interface, similar to previous reports. Therefore, considering $[\mathrm{Pt}(2-t)/\mathrm{Ni}(t)]_4$ multilayer as Pt/Ni bilayer is more reasonable than considering $[\mathrm{Pt}(2-t)/\mathrm{Ni}(t)]_4$ multilayer as a PtNi alloy.

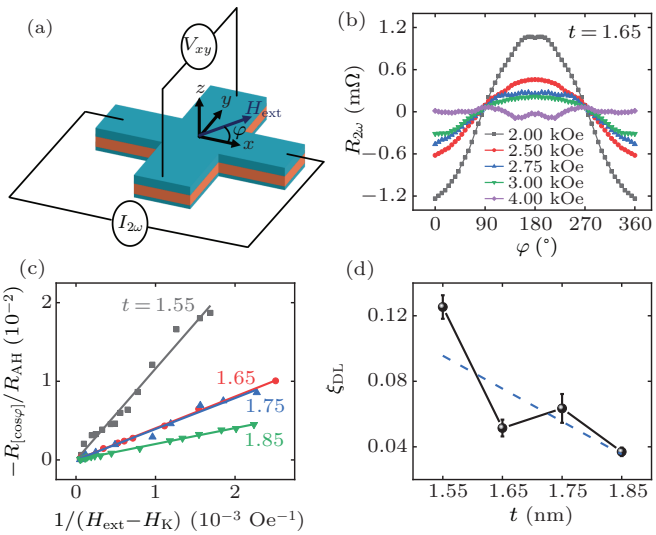



**Fig. 3.** (a) Schematic of the harmonic Hall measurement geometry. (b) The $\varphi$ dependence of $R_{2\omega}$ under different $H$. The inset illustrates the harmonic Hall measurement geometry (c) The $-R_{\cos\varphi}/R_{\mathrm{AH}}$ vs. $1/(H_{\mathrm{ext}}-H_{\mathrm{K}})$ curves at different $t$. (d) The $t$ dependence of $\xi_{\mathrm{DL}}$.

In comparison to Pt/Co and Pt/Fe bilayer films, the Pt/Ni system exhibits weaker interface SOC and magnetic proximity effects. Consequently, it experiences a smaller spin backflow phenomenon and spin memory loss at the interface.[35] As a result, in most cases, it is reasonable to consider that the damping-like torque in Pt/Ni systems primarily originates from the bulk spin Hall effect (SHE) of the heavy metal layer Pt, while the contribution from the Rashba effect at the interface is relatively minor. Furthermore, the interface Rashba field can be modulated by varying the number of periodic layers.[35] However, in this experiment, the number of periodic layers is fixed at 4, and only the thickness ($t$) is varied. Therefore, the contribution of the interface Rashba effect remains unchanged with the thickness $t$. Hence, our analysis can focus solely on the SHE contribution of the Pt layer.

To investigate the origin of the damping-like torque in the $[\mathrm{Pt}\ (2-t)/\mathrm{Ni}(t)]_4$ multilayer film structure, we can begin by examining a symmetrical three-layer film structure consisting of Pt/Ni/Pt, where the thicknesses of the top and bottom Pt layers are equal. Since the top and bottom Pt layers have equal thickness in the Pt/Ni/Pt three-layer film structure, and considering the SHE, the majority of the spin current contribution from the Pt layer is anticipated to have the same magnitude but opposite spin directions. Theoretically, this implies that the damping-like torque experienced by the middle Ni layer should cancel out due to the opposing spin currents. Consequently, in the $[\mathrm{Pt}(2-t)/\mathrm{Ni}(t)]_4$ multilayer film, only the top Ni layer is affected by the damping torque generated by the current flowing through the lower Pt layer. As a result, the damping-like switching efficiency of the Pt layer thickness within the range of 0.15–0.45 nm is expected to be extremely low.

However, as shown in the SOT tests and the second harmonic tests in Figs. 2 and 3, it has been demonstrated that the damping torque efficiency in the $[\mathrm{Pt}(2-t)/\mathrm{Ni}(t)]_4$ multilayer film is still very significant, close to the torque efficiency of Pt/Ni in the literature ($\sim 0.05$),[36] which means that the spin current from the Pt layer has not been completely offset. This means that the asymmetry between the top Ni/Pt and bottom Pt/Ni interfaces of the multilayer film is the key to the existence of a large damping torque in the symmetric three layers.

In the SOT study of Pt/Co multilayers with similar structures, there are different interface structures between Co/Pt and Pt/Co. The bottom Pt/Co exhibits a chemically sharp interface, but the top Co/Pt is slightly intermixed during the sputtering process, which may be the reason for the obvious damping-like torque.[37] This can also be used to explain the cause of symmetry breaking of the Pt/Ni system. Meanwhile, considering that the thickness of the Pt layer is relatively smaller compared to the Ni layer, as the Pt thickness increases, the increase in interface mixing may change the interface difference, which may also lead to $\xi_{\mathrm{DL}}$ increasing.

## 4. Conclusion

In this work, we have successfully fabricated a series of perpendicular magnetized $[\mathrm{Pt}(2-t)/\mathrm{Ni}(t)]_4$ multilayers and studied the SOTs as a function of the thickness of Ni layer. The damping-like SOT efficiency $\xi_{\mathrm{DL}}$ was extracted from an extended harmonic Hall measurement. We find that the $\xi_{\mathrm{DL}}$ increases with increasing the $t_{\mathrm{Pt}}/t_{\mathrm{Ni}}$ ratio due to pronounced contribution from the Pt layers. Our experimental results indicate that the perpendicularly magnetized Ni/Pt multilayers have a sizeable SOT efficiency which can be tuned by the $t_{\mathrm{Pt}}/t_{\mathrm{Ni}}$ ratio, and could be a promising material for the future SOT-MRAM.

## Data availability statement

The data that support the findings of this study are openly available in Science Data Bank at https://doi.org/10.57760/sciencedb.j00113.00126.

## Acknowledgements

Project supported by the National Key R&D Program of China (Grant No. 2021YFB3502400), the National Natural Science Foundation of China (Grant Nos. 52061135105, 12074025, 11834013, and 12274203), the CAS Project for

Yong Scientists in Basic Research (Grant No. YSBR-030), and the Key Research Project of Frontier Science of Chinese Academy of Sciences (Grant Nos. XDB44000000 and XDB28000000).

## References


[1] Shao Q M, Wang Z R and Yang J J 2022 *Nat. Electron.* **5** 67
[2] Wang J, Bai Y, Wang H, *et al.* 2022 *IEEE Transactions on Circuits and Systems I: Regular Papers* **69** 4535
[3] Ikegawa S, Mancoff F B, Janesky J and Aggarwal S 2020 *IEEE T. Electron Dev.* **67** 1407
[4] Zhu J G J and Park C 2006 *Materials today* **9** 36
[5] Ando Y 2015 *Jpn. J. Appl. Phys.* **54** 070101
[6] Apalkov D, Dieny B and Slaughter J M 2016 *Proc. IEEE* **104** 1796
[7] Lee S W and Lee K J 2016 *Proc. IEEE* **104** 1831
[8] Meng T, Ka S J and Shijie X 2020 *Adv. Mater.* **32** 2002607
[9] Yu J, Qiu X, Wu Y, *et al.* 2016 *Sci. Rep.* **6** 32629
[10] Zhang C, Takeuchi Y, Fukami S and Ohno H 2021 *Appl. Phys. Lett.* **118** 092406
[11] Safranski C, Sun J A T Z and Kent A D 2022 *Appl. Phys. Lett.* **120** 160502
[12] Lang L, Jiang Y, Lu F, *et al*. 2020 *Appl. Phys. Lett.* **116** 022409
[13] Liu T, Cai J W and Sun L 2012 *AIP Advances* **2** 032151
[14] Ikeda S, Miura K, Yamamoto H, *et al*. 2010 *Nat. Mater.* **9** 721
[15] Xu Y, Chen D, Tong S, *et al*. 2020 *Phys. Rev. Applied* **14** 034064
[16] Chen D, Xu Y, Tong S, *et al*. 2022 *Phys. Rev. Materials* **6** 014402
[17] Takahashi Y K, Ohnuma M and Hono K 2001 *Jpn. J. Appl. Phys.* **40** L1367
[18] Meng K K, Miao J, Xu X G, *et al*. 2016 *Phys. Rev. B* **94** 214413
[19] Liu L, Zhou C, Zhao T, *et al*. 2022 *Nat. Commun.* **13** 3539
[20] Nemoto H and Hosoe Y 2005 *J. Appl. Phys.* **97** 10J109
[21] Kamzin A S, Wei F L, Ganeev V R, *et al*. 2014 *Tech. Phys.* **59** 452
[22] Shin S C, Srinivas G, Kim Y S and Kim M G 1998 *Appl. Phys. Lett.* **73** 393
[23] Seki T, Tsujikawa M, Ito K, *et al*. 2020 *Phys. Rev. Materials* **4** 064413
[24] Zhou H, Wang C, Li Z, *et al*. 2020 *AIP Advances* **10** 015317
[25] Vedmedenko E Y, Kawakami R K, Sheka D D, *et al*. 2020 *J. Phys. D: Appl. Phys.* **53** 453001
[26] Ramaswamy R, Lee J M, Cai K M and Yang H 2018 *Appl. Phys. Rev.* **5** 031107
[27] Golod T, Rydh A and Krasnov V M 2011 *J. Appl. Phys.* **110** 033909
[28] Xue F, Lin S J, Dc M, *et al*. 2021 *Appl. Phys. Lett.* **118** 042405
[29] Zhu L, Ralph D C and Buhrman R A 2021 *Appl. Phys. Rev.* **8** 031308
[30] Liu T X, Wang Z H, Wang M, *et al*. 2022 *Chin. Phys. B* **31** 107501
[31] Kim S, Jang P H, Kim D H, *et al*. 2017 *Phys. Rev. B* **95** 220402
[32] Zhang H C, Ma X Y, Jiang C P, *et al.* 2022 *J. Semicond* **43** 102501
[33] Martini M, Avci C O, Tacchi S, *et al*. 2022 *Phys. Rev. Appl.* **17** 044056
[34] Zhu L, Zhu L and Buhrman R A 2021 *Phys. Rev. Lett.* **126** 107204
[35] Hayashi H, Musha A, Sakimura H and Ando K 2021 *Phys. Rev. Res.* **3** 013042
[36] Chen L N, Zhan X, Zhou K Y, *et al*. 2022 *Phys. Rev. Appl.* **17** 064041
[37] Huang K F, Wang D S, Lin H H and Lai C H 2015 *Appl. Phys. Lett.* **107** 232407